

CONTEXTUAL ENERGY EQUALIZATION AND GAMMA CORRECTION-BASED CONTRAST ENHANCEMENT WITH CLIPPING CONSTRAINT

¹Chian-Huey Liaw (廖千慧) ²Chiou-Shann Fuh (傅楸善)

¹ Department of Electrical Engineering,

National Taiwan University of Science and Technology, Taipei, Taiwan,

² Department of Computer Science and Information Engineering,

National Taiwan University, Taipei, Taiwan,

*E-mail: M11107426@mail.ntust.edu.tw fuh@csie.ntu.edu.tw

ABSTRACT

This paper proposes a novel approach for enhancing image contrast by leveraging contextual energy equalization and gamma correction with a clipping constraint. Traditional contrast enhancement techniques often suffer from issues such as loss of image details and over-amplification of noise. To address these challenges, the proposed method utilizes contextual information to adaptively equalize the image's energy distribution while applying gamma correction to enhance contrast. Additionally, a clipping constraint is imposed to avoid excessive enhancement and preserve image integrity. Experimental results demonstrate that the proposed approach effectively enhances contrast, improves visual quality, and retains important image details. Moreover, the integration of contextual energy equalization, gamma correction, and clipping constraint provides flexibility and adaptability, making it suitable for various image processing applications. The proposed method exhibits promising potential in enhancing contrast in real-world images.

Keywords: *Image contrast enhancement, Contextual energy equalization, Clipping constraint, Color image, Hopfield neural network, Gamma correction.*

1. INTRODUCTION

The enhancement of image contrast is a fundamental task in various image processing applications, such as computer vision, medical imaging, and surveillance systems. It plays a crucial role in improving visual perception, extracting meaningful information, and facilitating subsequent analysis tasks. However,

traditional contrast enhancement techniques often face challenges in simultaneously preserving image details and avoiding the amplification of noise and artifacts.

To address these limitations, this paper introduces a novel approach for image contrast enhancement based on contextual energy equalization and gamma correction with a clipping constraint. Contextual information has been proven to be valuable in image processing tasks as it considers the local characteristics and relationships among neighboring pixels. By incorporating contextual energy equalization, the proposed method adaptively adjusts the energy distribution of the image to enhance contrast while preserving important image details.

Gamma correction is employed as an additional step to further improve the perceptual quality of the enhanced image. By applying a nonlinear mapping, gamma correction enhances the visibility of image details in both the dark and bright regions. Moreover, to ensure the output remains visually pleasing and retains the overall image integrity, a clipping constraint is introduced to prevent over-enhancement and limit the amplification of noise.

The effectiveness of the proposed method is evaluated through extensive experiments on various images with different levels of contrast distortion. Quantitative metrics such as Natural Image Quality Evaluator (NIQE ↓, the lower the better) and Blind Referenceless Image Spatial Quality Evaluator (BRISQUE ↓, the lower the better) are employed to assess the quality of the enhanced images. Additionally, qualitative evaluations are conducted to visually compare the results against existing contrast enhancement techniques.

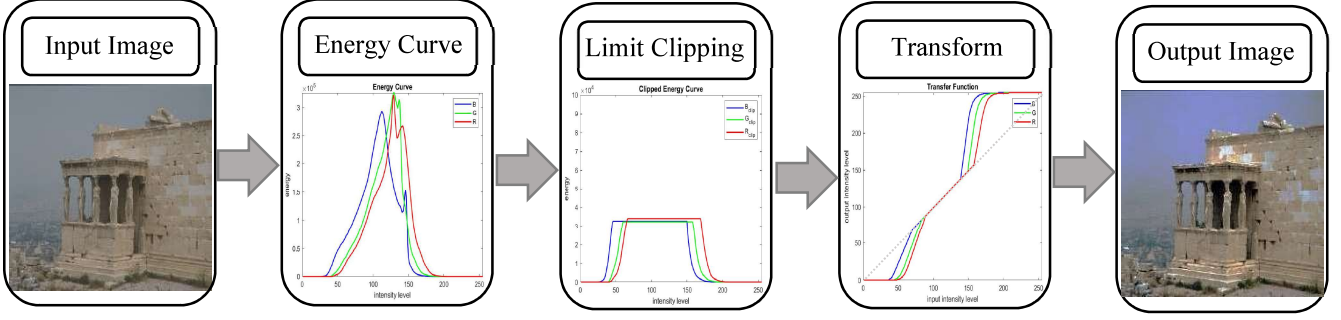


Fig 1. Illustration of the proposed algorithm.

The rest of the paper is organized as follows: Section II provides a review of related works in the field of image contrast enhancement. Section III presents the proposed method in detail, including the contextual energy equalization, clipping constraint, and gamma correction. Experimental results and analysis are presented in Section IV. Finally, Section V concludes the paper, highlighting the contributions and potential future research directions.

Overall, this paper aims to provide a comprehensive and effective solution for image contrast enhancement by leveraging contextual energy equalization, gamma correction, and a clipping constraint. The proposed method addresses the limitations of traditional techniques and offers improved visual quality while preserving image integrity.

2. RELATED WORK

2.1. Histogram Equalization

The conventional Histogram Equalization (HE) process consists of two main steps. Firstly, the histogram is computed by counting the occurrences of each intensity level in the image. Consider an image I_o , which has dimensions $m \times n$ and contains N pixels. The gray levels of the image range from 0 to $L-1$. Generally, the intensity contained in the 8bits image is 0 to 255. The histogram is computed as $H(l)=n(l)$, where l is the intensity level and $n(l)$ is the number of the pixel at that intensity level. This provides information about the distribution of intensity values across the image. Secondly, a transfer function is generated based on the Probability Density Function (PDF) and Cumulative Distribution Function (CDF) derived from the histogram. The PDF represents the normalized histogram and is defined as

$$PDF(l) = \frac{n(l)}{N}, \quad \text{for } l = 0, 1, 2, \dots, L-1$$

while the CDF is obtained by cumulatively summing the PDF values and is defined as

$$CDF(l) = \sum_{i=0}^l PDF(i), \quad \text{for } l = 0, 1, 2, \dots, L-1$$

The transfer function maps the input intensity values to output intensity values $T(l)$, effectively redistributing the intensity levels l to achieve a more balanced histogram. The transfer function is as follows

$$T(l) = (L - 1) \times CDF(l)$$

This transformation aims to spread out the intensity values across the entire dynamic range, enhancing the overall image appearance. The scaling of the CDF ensures that the output intensities cover the full range of possible values.

2.2. Gamma Correction

Luminance plays a crucial role in image processing as it greatly influences the perception of details. However, imaging devices often introduce non-linear effects that impact the overall brightness of an image. To address this, gamma correction is employed as a non-linear operation that enhances the brightness of an image. Gamma correction is defined by a power law expression as follows

$$V_{out} = CV_{in}^\gamma$$

where the output brightness value (V_{out}) is determined based on the input brightness value (V_{in}) using a gamma value (γ), both the input and output values are non-negative real numbers. C is a constant. Typically, when A is set to 1, the input and output values range between 0 and 1. In the case of $\gamma < 1$, the gamma correction expands the darker regions of an image, resulting in an overall brighter image. Conversely, when $\gamma > 1$, the gamma correction expands the brighter regions, leading to a darker image overall. This process allows for the adjustment of brightness levels to achieve the desired visual effect.

By applying the inverse of the gamma correction process, the original brightness values can be recovered.

$$V_{in} = V_{out}^{\frac{1}{\gamma}}$$

The application of gamma correction is particularly beneficial in removing non-linear effects during the

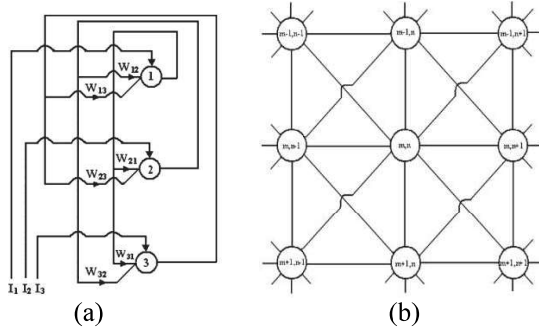


Fig 2. Illustration of the Hopfield neural network (a) Hopfield Network Model architecture. (b) Second-order topological network.

preprocessing stage of various applications, including digital photography, image processing, and computer vision. It allows for improved visual quality and ensures more accurate representation of the original scene.

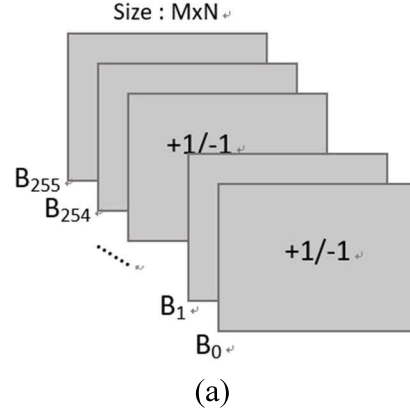
In this paper, a technique is proposed for estimating the gamma correction factor without any prior information or knowledge about the ambient light or imaging device. The basic approach leverages the fact that the gamma correction factor is based on the average brightness value and is used to adjust the brightness of an image.

3. CONTEXTUAL ENERGY EQUALIZATION AND CLIPPING CONSTRAINT

The proposed method is visually depicted in Figure 1, illustrating its three main steps: energy curve computation, limit clipping and Transfer Function (TF) generation. In the following subsections detail the computation of the energy curve and the energy curve equalization process.

3.1. Energy Curve

The energy curve of the image is derived from a modified Hopfield Neural Network (HNN) architecture [3, 4, 5]. The Hopfield neural network is composed of multiple neurons, each of which is connected to each other through different synaptic weights in Fig.2(a). It is a recurrent neural network with feedback connection neurons from output to input. Using the improved Hopfield neural network, each neuron is regarded as each pixel in the image, and each pixel is connected to the nearest neighbor pixel, and the corresponding energy is calculated. Synaptic weights are also modified in the modified Hopfield neural network. These weights are fixed at "1" or "0". For pixels located in neighboring regions, the synaptic weight was assigned '1'; otherwise, it was fixed to '0'. The complete state of the network is represented by an energy function computed using the network architecture. The energy curve consists of peaks and troughs similar to a histogram and is calculated by obtaining the distribution of pixels in the neighborhood



1	1	1	-1	-1	-1
1	1	-1	1	-1	-1
-1	-1	-1	1	1	1
1	1	1	-1	1	1
1	-1	1	-1	1	-1
-1	1	-1	1	-1	-1
-1	1	1	1	-1	-1

Fig 3. Visual presentation of B_i matrix computation. (a) Structure of B_i matrix. (b) Sample entry values in B_i matrix.

of the image. For images with the following changes, the modified HNN completes the entire network structure and calculates the energy value for each intensity level. The energy curve calculation process is as follows:

Consider an image I with dimensions $m \times n$ where the pixel value at location (i, j) is given by $I(i, j)$ ($0 \leq I(i, j) \leq L-1$). To account for the spatial correlation between pixels, a neighborhood system N with order d at a spatial location (i, j) is defined as $N_{i,j}^d = \{(i+u, j+v) | (u, v) \in N^d\}$. Pixels included in N^d take spatial correlation into account. Depending on the value of d , different neighborhood conditions can be considered. Since the second-order neighborhood system is considered in this work, eight surrounding pixels are considered, namely, $N^2 = \{(\pm 1, 0), (0, \pm 1), (1, \pm 1), (-1, \pm 1)\}$. A second-order system in Fig. 2(b) is considered because it is connected to all surrounding pixels. Increasing the order will increase the complexity of energy calculation. The term modified Hopfield neural network is used because the values of the synaptic weights are modified to be 1 or 0. For neurons located in the neighborhood ($N_{i,j}^d$), connection weights are assigned 1, while for neurons outside the neighborhood ($N_{i,j}^d$), connection weights are assigned zero. This makes each neuron only connect to its neighbors, which makes the result only depend on the neighbors. This process

essentially models the network and examines the spatial contextual properties of the pixel information. [7] computes the energy curves and presents the corresponding normalized energy curves for the 3×3 , 5×5 , and 7×7 neighborhood sizes. Increasing the neighborhood size results in smaller bias gain and increases computation time compared to smaller neighborhood sizes. Therefore, in this paper, a neighborhood size of 3×3 is considered instead of larger neighborhood sizes.

The calculation of the energy function involves the matrix B_l ($B_0, B_1, B_2, \dots, B_{255}$), whose entries are "+1" or "-1" based on the intensity values of the original image. The size of matrix B_l is also similar to the input image. For a particular intensity level (l), the entries of the matrix B_l are computed as

$$B_l(i, j) = \begin{cases} +1, & \text{if } I(i, j) > l \\ -1, & \text{else} \end{cases}$$

The structure of the matrix B_l and its internal elements are shown in Figure 3. From the matrix B_l , the energy curve of a particular intensity level l is calculated as

$$E^f(l) = - \sum_{i=0}^m \sum_{j=0}^n \sum_{p,q \in N_{i,j}^d} B(i, j) \times B(p, q) \\ + \sum_{i=0}^m \sum_{j=0}^n \sum_{p,q \in N_{i,j}^d} C(i, j) \times C(p, q)$$

The energy curve consists of different energy values for different intensity values, where ' l ' represents the grayscale value and the value of ' f ' represents image's depth, varies from 1 to 3 for color images and is fixed at ' l ' for gray images. The matrix $C = 1 \ \forall(i, j)$ incorporated into the equation to realize the energy of the pixel, which is a non-negative value ($E^f \geq 0$). For a particular value of l , if all pixel values are either larger or smaller, the energy of that gray level becomes minimum. The energy curve has a minimum at the point where the histogram has a zero value. The calculated energy curve of an image is shown in Figure 4, which follows the range of the histogram. Energy curves look smoother than histograms. The energy value at each intensity level depends on neighboring pixels; therefore, the value at each intensity location is not similar to the image's histogram.

3.2. Clipping and Sectioning of the Energy Curve

In order to limit the enhancement rate, the calculated energy is bounded within the clipping limit. Most algorithms use the mean or median as clipping limit. In a symmetric data distribution, the mean and median are equal. If the data are distributed asymmetrically

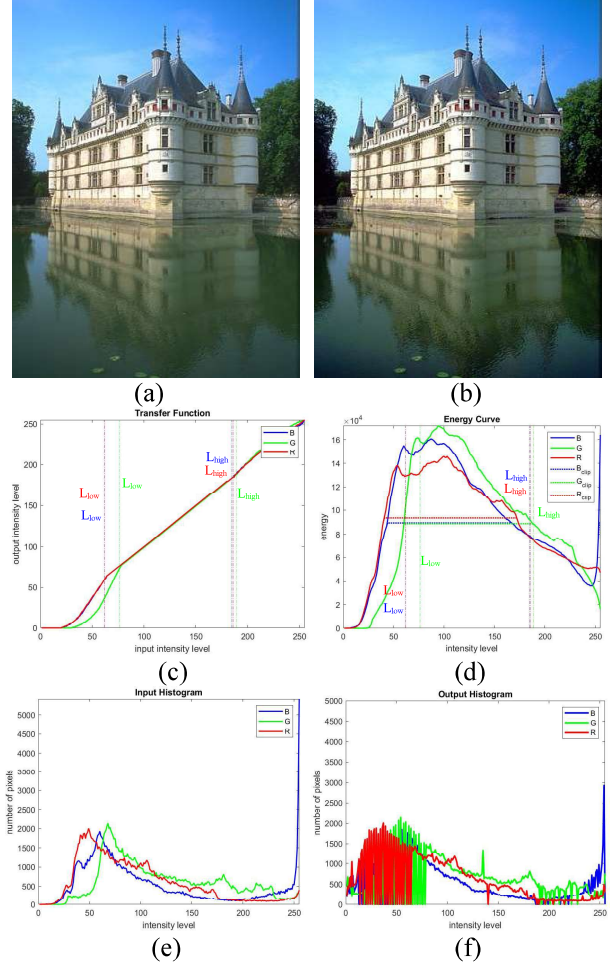


Fig 4. Results for a sample image (a) Input image (b) Enhanced image (c) Energy curve (clipped and without clipped) and equalization process (d) Mapping function (e) Input histogram and (f) Output histogram.

(positive/negative skew), the mean and median are not equal. Here, the proposed algorithm provides the flexibility to handle these changes in the data distribution. It does this by selecting the clipping of the input energy curve by mean of the median and mean of the intensity. The clipping limit is calculated as the average of the median and mean intensity values of the energy curve and calculated as

$$C_{median} = median(E^f(l))$$

$$C_{mean} = mean(E^f(l))$$

$$C_{clip} = \frac{C_{median} + C_{mean}}{2}$$

The energy curve is clipped using the computed clipping limit as

$$\hat{E}^f(l) = \begin{cases} C_{clip}, & \text{if } E^f(l) \geq C_{clip} \\ E^f(l), & \text{else} \end{cases}$$

Where $\hat{E}^f(l)$ is the clipped energy curve. Calculated as energy values above the calculated clipping limit (C_{clip}) are replaced by C_{clip} , leaving the rest unchanged. And then the clipped energy curve is divided into three regions according to the standard deviation (SD) and is calculated as follows

$$SD = \sqrt{\frac{\sum_{l=0}^{L-1} (l - \hat{E}^f_{mean})^2 \times \hat{E}^f(l)}{\sum_{l=0}^{L-1} \hat{E}^f(l)}}$$

where \hat{E}^f_{mean} is the mean of the clipped energy curve, which is calculated as follows

$$\hat{E}^f_{mean} = \frac{\sum_{l=0}^{L-1} \hat{E}^f(l) \times l}{\sum_{l=0}^{L-1} \hat{E}^f(l)}$$

Based on the SD value, the lower and upper limits are computed to split the energy curve. The lower (L_{low}) and upper (L_{high}) limits are computed as

$$L_{low} = \hat{E}^f_{mean} - SD$$

$$L_{high} = \hat{E}^f_{mean} + SD$$

The energy curve is spliced into three sub-energy regions. The first sub-energy curve ranges from 0 to L_{low} , the second sub-energy curve ranges from $L_{low} + 1$ to L_{high} , and the third sub-energy curve ranges from $L_{high} + 1$ to $L - 1$. The standard deviation is chosen as the splicing parameter to cover the image's maximum energy region. The middle sub-energy curve conceals the maximum energy region, which helps conserve the image's mean energy. The computed energy curves, along with the clipping limits and lower and upper bounds for the sub-division of energy curves.

3.3. Energy Curve Equalization

During this process, sub-energy curves are generated and individually equalized before being combined to form the final transfer function. The computation of the transfer function follows a similar procedure to that of Histogram Equalization (HE) and involves three main steps: calculating the Probability Density Function (PDF), deriving the Cumulative Distribution Function (CDF) from the PDF , and generating the transfer function.

The PDF s for the sub-energy curves are denoted as $PDF_L(l)$, $PDF_M(l)$, and $PDF_U(l)$ are defined as

$$PDF_L(l) = \frac{\hat{E}^f(l)}{n_L} \quad \text{for } 0 \leq l \leq L_{low}$$

$$PDF_M(l) = \frac{\hat{E}^f(l)}{n_M} \quad \text{for } L_{low} + 1 \leq l \leq L_{high}$$

$$PDF_H(l) = \frac{\hat{E}^f(l)}{n_H} \quad \text{for } L_{high} + 1 \leq l \leq L - 1$$

where n_L , n_M , and n_H are represent the absolute energy level in the three sub-energy curves, respectively. These values indicate the magnitude of energy within each sub-energy curve. These PDF s represent the probability distributions of the lower, middle, and upper portions of the energy curve, respectively. They provide valuable insights into the distribution of pixel intensities within each sub-energy curve and guide the subsequent equalization process.

The CDF s represents the accumulated probabilities of encountering pixel intensities within the sub-energy curve. It provides valuable information about the distribution and relative frequencies of pixel values in the image and is defined as follows

$$CDF_L(l) = \sum_{k=0}^l PDF_L(k) \quad \text{for } 0 \leq l \leq L_{low}$$

$$CDF_M(l) = \sum_{k=L_{low}+1}^l PDF_M(k) \quad \text{for } L_{low} + 1 \leq l \leq L_{high}$$

$$CDF_H(l) = \sum_{k=L_{high}+1}^l PDF_H(k) \quad \text{for } L_{high} + 1 \leq l \leq L - 1$$

Using the Cumulative Distribution Functions (CDF s) obtained from the sub-energy curves, the transfer function for each curve is generated as follows

$$T_L(l) = L_{low} \times CDF_L(l)$$

$$T_M(l) = (L_{low} + 1) + (L_{high} - (L_{low} + 1)) \times CDF_M(l)$$

$$T_U(l) = (L_{high} + 1) + ((L - 1) - (L_{high} + 1)) \times CDF_U(l)$$

The final Transfer Function (TF) is obtained by merging the three individual functions together as shown below.

$$T(l) = T_L(l) + T_M(l) + T_U(l)$$

The proposed method employs a Transfer Function (TF), derived from above equations, to enhance the contrast of the input image. This transfer function serves as a mapping between the input intensity values and the corresponding output intensity values in the contrast-enhanced image. It can be visualized as a lookup table, where each input intensity value is transformed to its corresponding output intensity value.

3.4. Gamma Correction

The average luminance is a simple metric that can be computed quickly. In this study, we propose a basic method that estimates an appropriate gamma based on the average luminance. While the average luminance may not capture all the information of an image, it serves as a good indicator when selecting a sample between

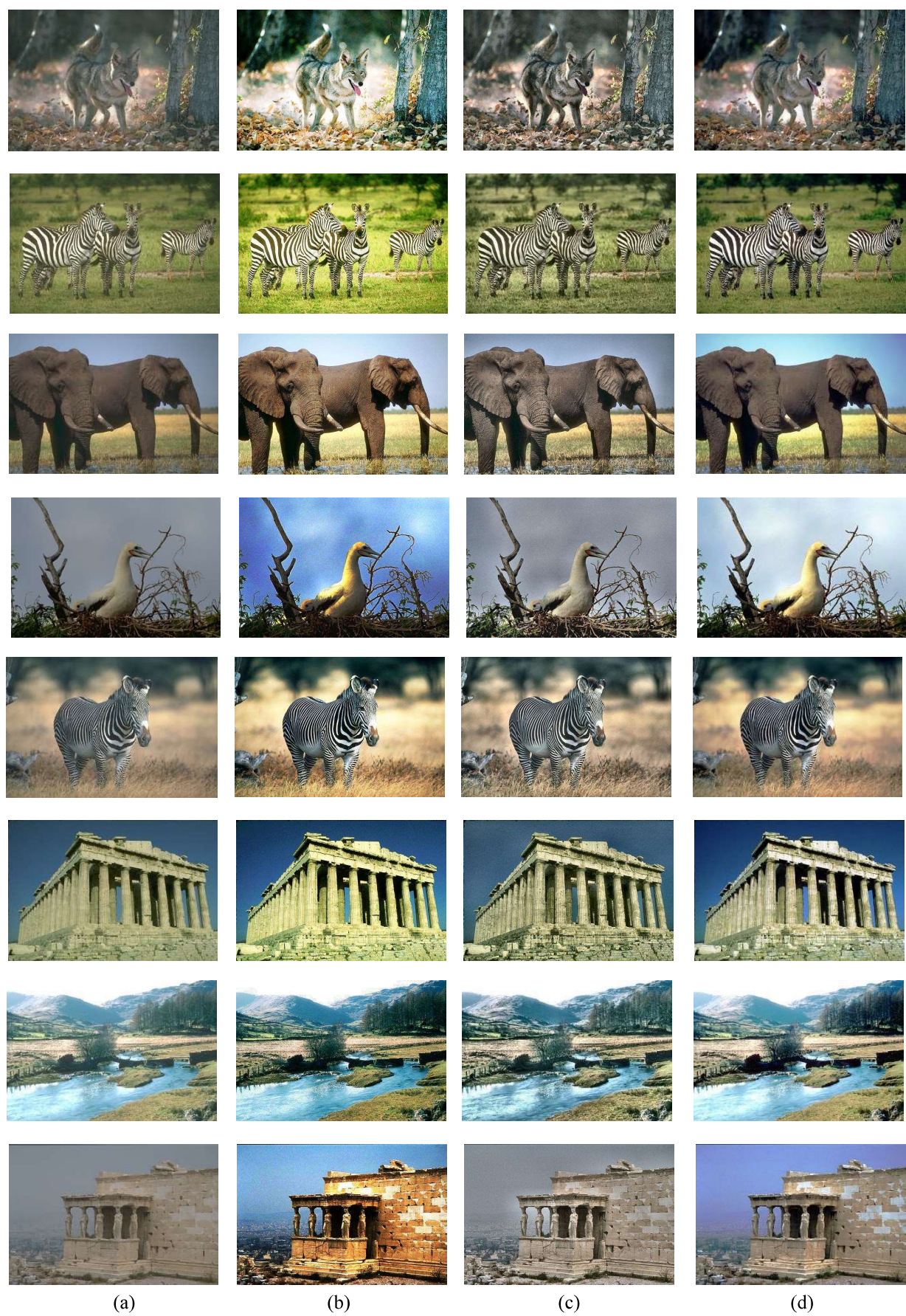


Fig 5. Visual comparison of input and enhanced images. From left to right indicates the (a) Input image, (b) HE [8], (c) CLAHE [9] and (d) Proposed method.

brightness values in the histogram. We present a method that performs correction based on the average luminance. The global gamma for gamma correction can be chosen by considering this power. The optimal contrast in an image is typically achieved at a luminance of 0.5, thus no correction is applied when the overall luminance of the image falls within the range of 0.4 to 0.6. If the overall luminance is below 0.4, setting gamma to a value less than 1 expands the dark regions, resulting in a brighter image. Conversely, if the overall luminance is above 0.6, setting gamma to a value greater than 1 expands the bright regions, enhancing the image contrast.

We take the average brightness as a basis, and then estimate the gamma value according to the following equation

$$V_{out} = V_{in}^\gamma$$

$$\gamma = \begin{cases} \frac{\text{ceil}(\log(Avg))}{\log(Avg)} & \text{for } Avg < 0.4 \\ 1 & \text{for } 0.4 \leq Avg \leq 0.6 \\ \frac{\text{floor}(\log(Avg))}{\log(Avg)} & \text{for } Avg > 0.6 \end{cases}$$

where Avg is the average of the clipped energy curve, which is calculated as below:

$$Avg = \frac{\sum_{l=0}^{L-1} \hat{E}^f(l) \times l}{\sum_{l=0}^{L-1} \hat{E}^f(l)}$$

The estimated gamma value is applied to enhance all pixels in the output image. Subsequently, the same enhancement method is applied to the entire input image. This ensures that every pixel in the output image benefits from the estimated gamma value, resulting in an overall enhancement of the image.

4. EXPERIMENTAL RESULTS

In this section, various experiments were conducted to validate the proposed algorithm. The experiments involved images with significant contrast variations under different lighting conditions. It was important to compare the performance against other histogram-based algorithms. Such comparisons were justified given that the performance of these histogram-based algorithms has been previously verified for contrast enhancement tasks.

The experimental results, as shown in Figure 5, demonstrate a visual comparison between the input image and the enhanced image. These comparisons clearly validate the effectiveness of the proposed algorithm in enhancing image contrast. In addition, objective image quality assessment metrics such as NIQE and BRISQUE were used for comparison, as shown in Tables 1 and 2. Both metrics provide a quantitative

Table 1. NIQE ↓ Values for the Different Methods.

NIQE	Original	HE[8]	CLAHE[9]	Proposed
Img1	3.466	3.593	3.71	3.187
Img2	3.233	3.419	3.146	3.005
Img3	2.78	3.694	3.263	2.677
Img4	2.54	2.821	3.37	2.423
Img5	2.473	2.36	2.467	2.433
Img6	3.592	4.193	3.929	3.472
Img7	3.278	3.135	3.547	3.178
Img8	2.903	2.768	2.82	2.851
Img9	3.616	4.126	4.587	3.765
Img10	3.428	3.892	3.233	3.447
Img11	3.308	3.366	3.016	3.139
Img12	4.765	4.706	4.097	4.286
Img13	2.01	3.581	2.5	2.296
Img14	2.835	2.819	2.342	2.616
Img15	3.085	2.695	2.143	2.31
Img16	2.599	3.291	2.367	2.202
Img17	2.704	3.404	2.719	2.673
Img18	8.123	5.836	5.515	6.836
Average	3.374	3.539	3.265	3.155

Table 2. BRISQUE ↓ Values for the Different Methods.

BRISQUE	Original	HE[8]	CLAHE[9]	Proposed
Img1	26.438	28.479	30.248	29.611
Img2	23.447	26.189	13.245	15.73
Img3	25.687	39.365	35.962	24.114
Img4	29.31	22.15	1.69	30.61
Img5	19.32	21.717	14.63	20.443
Img6	14.476	27.074	26.067	5.128
Img7	16.668	29.077	31.944	16.202
Img8	22.361	28.75	10.729	20.452
Img9	30.411	32.731	36.207	30.47
Img10	17.681	19.981	20.771	17.465
Img11	8.219	22.264	16.438	7.885
Img12	16.29	34.122	37.019	5.401
Img13	7.691	17.658	20.612	7.185
Img14	7.929	25.052	11.345	4.137
Img15	27.401	16.452	14.245	30.598
Img16	15.846	14.346	3.251	6.648
Img17	13.907	18.152	23.944	23.596
Img18	43.492	42.177	42.109	41.002
Average	20.365	25.874	21.692	18.704

evaluation of image quality without the need for reference images, and lower scores indicate better image quality. The results of the experiment further emphasize the superiority of the energy curve-based approach over traditional histogram-based methods in addressing the challenges of contrast enhancement.

The objective evaluation using NIQE and BRISQUE metrics supports the visual comparisons and confirms the improved quality achieved by the proposed algorithm. These findings contribute to the overall validation and effectiveness of the energy curve-based method in enhancing image contrast.

5. CONCLUSION

Our study introduces an innovative approach for image contrast enhancement that leverages contextual energy equalization, gamma correction, and a clipping constraint. By incorporating contextual information and considering the local characteristics, our method offers a promising solution to enhance contrast while preserving image integrity. The experimental results demonstrate the effectiveness of our approach and its potential in various image processing applications.

REFERENCES

- [1] K. Srinivas, A. K. Bhandari, and A. Singh, "Exposure-based energy curve equalization for enhancement of contrast distorted images." *IEEE Transactions on Circuits and Systems for Video Technology*, vol. 30, no. 12, pp. 4663-4675, 2019.
- [2] G. Susmita, et al. "A context-sensitive technique for unsupervised change detection based on Hopfield-type neural networks." *IEEE Transactions on Geoscience and Remote Sensing*, vol. 45, no. 3, pp. 778-789, 2007.
- [3] A.K. Bhandari, A. Singh, I.V. Kumar, "Spatial context energy curve-based multilevel 3-D Otsu algorithm for image segmentation," *IEEE Trans. Syst. Man Cybern. Syst.*, vol. 51, no. 5, pp. 2760-2773, 2019.
- [4] S. Ghosh, L. Bruzzone, S. Patra, F. Bovolo, and A. Ghosh, "A contextsensitive technique for unsupervised change detection based on Hopfield-type neural networks," *IEEE Trans. Geosci. Remote Sens.*, vol. 45, no. 3, pp. 778-788, 2007.
- [5] S. Patra, R. Gautam, and A. Singla, "A novel context sensitive multilevel thresholding for image segmentation," *Appl. Soft Comput.*, vol. 23, pp. 122-127, 2014.
- [6] Babakhani, Pedram, and Parham Zarei. "Automatic gamma correction based on average of brightness." *Advances in Computer Science: an International Journal*, vol. 4, no.18 , pp. 156-160, 2015.
- [7] Srinivas, Kankanala, Ashish Kumar Bhandari, and Pulli Kishore Kumar. "A context-based image contrast enhancement using energy equalization with clipping limit." *IEEE Transactions on Image Processing*. vol. 30. pp. 5391-5401, 2021.
- [8] R. E. W. Rafael C. Gonzalez, Digital Image Processing, 3rd ed. Upper Saddle River, NJ, USA: Prentice-Hall, 2008.
- [9] P. S. Heckbert and Karel, Graphics Gems IV. Gurgaon, Haryana: AP Professional, 1994.
- [10] Shi, Y., Yang, J. and Wu, R. "Reducing Illumination Based on Nonlinear Gamma Correction," *In Proc. 310*, vol. 24, no. 4, 2011.
- [11] Chen, S. D. and Ramli, A. R. "Minimum mean brightness error bihistogram equalization in contrast enhancement", *IEEE Transactions on Consumer Electronics*, vol. 49, no. 4, pp. 1310-1319, 2003.
- [12] Asadi Amiri, S., Hassanpour ,H. and Pouyan, A. "Texture Based Image Enhancement Using Gamma Correction", *Middle-East Journal of Scientific Research* , vol. 6, pp. 569-574. 2010.
- [13] Babakhani, P. "automatic gamma correction based on average and deviation from center of histogram". *2th International Conference on Advances in Engineering and Basic Sciences*, pp. 76-82, 2015.
- [14] N. Ponomarenko, V. Lukin, A. Zelensky, K. Egiazarian, M. Carli, and F. Battisti, "TID2008-a database for evaluation of full-reference visual quality assessment metrics," *Adv. Mod. Radioelectron.*, vol. 10, no. 4, pp. 30-45, 2009.
- [15] N. Ponomarenko et al., "Image database TID2013: Peculiarities, results and perspectives," *Signal Process., Image Commun.*, vol. 30, pp. 57-77, 2015.
- [16] D. M. Chandler, "Most apparent distortion: Full-reference image quality assessment and the role of strategy," *J. Electron. Imag.*, vol. 19, no. 1, 2010.
- [17] D. Martin, C. Fowlkes, D. Tal, and J. Malik, "A database of human segmented natural images and its application to evaluating segmentation algorithms and measuring ecological statistics," *in Proc. 8th Int. Conf. Comput. Vis.*, vol. 2, pp. 416-423, 2001.